Available online at www.sciencedirect.com
SCIENCE DIRECT®
ELSEVIER
International Journal of Solids and Structures 42 (2005) 5669–5682
INTERNATIONAL JOURNAL OF SOLIDS and STRUCTURES
www.elsevier.com/locate/ijsolstr

Stick-slip chaos detection in coupled oscillators with friction

J. Awrejcewicz *, D. Sendkowski

Technical University of Lodz, Department of Automatics and Biomechanics, 1/15 Stefanowskiego St., 90-924 Lodz, Poland

Received 8 February 2005
Available online 26 April 2005

Abstract

We consider two coupled oscillators with negative Duffing type stiffness which are self (due to friction) and externally (harmonically) excited. The fundamental solutions of the homoclinic orbit are constructed. Then, the Melnikov–Gruendler approach is used to define the Melnikov's function including smooth and stick-slip chaotic behaviour. Theoretical considerations are supported by numerical examples.

PACS: 05.45.Jn

Keywords: Chaos; Coulomb friction; Melnikov's method

1. Introduction

There exist a vast research devoted to analysis of low and high dimensional systems with friction. Some fundamental problems of non-smooth dynamical systems with friction are addressed for example, in references (Awrejcewicz and Delfs, 1990; Awrejcewicz and Delfs, 1990; Fečkan, 1999; Kunze, 2000; Lamarque and Bastien, 2000; Pfeiffer and Hajek, 1992; Stelter, 1992). However we are not going to cite many of them, but a reader may go through over 400 bibliography items devoted to non-smooth regular and chaotic dynamics included in the recent monograph by Awrejcewicz and Lamarque (2003). Beginning from the pioneering work of Melnikov (1963), the Melnikov-like approaches spread into different branches of science. We briefly address the Melnikov-like techniques to predict the onset of chaos in systems governed by ODEs or maps. For example, in reference (Balasuriya et al., 2003) the Melnikov function (integral) is successfully applied in fluid particle kinematics analysis in weakly perturbed integrable dynamical systems. The method

* Corresponding author. Tel./fax: +48 42 6312225.
E-mail address: awrejcew@p.lodz.pl (J. Awrejcewicz).

0020-7683/$ - see front matter
doi:10.1016/j.ijsolstr.2005.03.018

proposed by Melnikov allows also to predict the onset of chaos via homoclinic (or heteroclinic) tangencies in periodically perturbed $2D$ flows (see also Holmes and Mardsen, 1982; Wiggins, 1989). An existence of transversal homoclinic orbits of systems of singularly perturbed two first order differential equations using the exponential dichotomies is illustrated and discussed in Weiyao and Jiaowan (1999). The exponential dichotomy and a unified geometrical approach to calculate the Melnikov vector function assuming the existence of transversal homoclinic points for high-dimensional maps with a saddle connection are studied in Sun (1996). A splitting of separatrices for high-frequency perturbations of a planar Hamiltonian system using the Melnikov technique is also examined (see Gelfreich, 1997). In reference Smith (1998) it is shown that although the original Melnikov's approach correctly estimates the parameter values for the bifurcation and transverse intersections of separatrices and manifolds, it does not correctly approximate solutions in a neighbourhood of the associated fixed point of the homoclinic orbit. In the latter paper a multiple scales technique, in which inner solutions are matched with a regular outer solution, has been proposed. Finally, we finish our brief review of recent modifications and for extensions of the Melnikov'a original work addressing the results obtained by Fathi and Salam (1987). In the mentioned reference, an extension of the Melnikov approach to a class of highly dissipative systems is proposed, and the obtained results are illustrated using numerical simulations. There are several extensions of the Melnikov's method (Holmes and Mardsen, 1982; Sanders, 1980) however, mainly Gruendler's work Gruendler (1985) served for us as the basic reference to start with a construction of a homoclinic orbit in our $4D$ mechanical system perturbed by friction and harmonic excitation, and then to derive the associated Melnikov's function. It is worth noticing that an important opened problem of the Melnikov's approach relies on its extension into analysis of higher order dynamical systems. This problem seems to be unsolved since it is difficult to establish a priori a homoclinic orbit associated with a highly dimensional system considered. It is needless to say that a prediction of chaos in an analytical way in non-smooth objects modelled as systems in R^4 plays a crucial role for both theoretical and applicable reasons. A key role of research carried out in this direction plays the paper by Awrejcewicz and Holicke (1999), where a chaotic threshold for both smooth and stick-slip chaotic behaviour in one degree-of-freedom system with friction has been obtained using directly the Melnikov's technique. On the other hand, it was impossible to extend directly the original Melnikov's method devoted to analysis of an analytic system in R^2. Therefore, we have applied the Gruendler extension of the Melnikov's method to R^4, which is further referred as the Melnikov–Gruendler approach. However, in the cited Gruendler's work Gruendler (1985) again an emphasis of C^2 systems is given. In contrary, in our research we extend the results obtained earlier (see Awrejcewicz and Holicke, 1999) to R^4. Although we do not give a rigorous definitions and proofs of a C^n vector field on R^n, but we show the computations of related integrals yielding a being sought chaotic threshold defined by the approproate Melnikov's function. Furthermore, a reduction of the obtained Melnikov integrals to those associated with previously considered one degree-of-freedom mechanical system and the illustrated numerical examples indicate a validity of our approach.

2. The analysed system

The analysed mechanical object consists of two stiff bodies with the masses m coupled via nonlinear springs in the way shown in Fig. 1.

Note that when the system is autonomous, i.e. $\Gamma = 0$, the self-excited oscillations appear, which are generated by frictional characteristics. The latter ones possess a decreasing part versus a relative velocity between both bodies and the tape moving with a constant velocity w. Although this problem belongs to classical ones and has been studied by vast number of researchers, an attempt to formulate threshold for chaos occurence in the analytical way failed. In what follows we show how to solve this problem using the Melnikov technique applied to our discontinuous system. It is also recommended to be familiar with the reference Awrejcewicz and Holicke (1999), where a similar like approach has been applied to predict

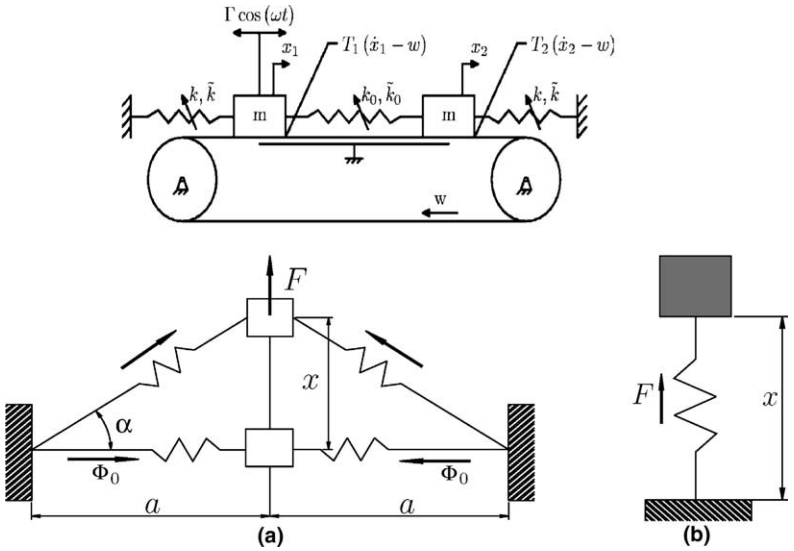

Fig. 1. The analysed system. (a) Negative stiffness system. (b) Equivalent system.

chaos in a similar like system, but with one degree-of-freedom. The analyzed system is conservative when the friction and the excitation equals to zero. Hence, the Hamiltonian of the system (see Fig. 1) has the following form:

$$H = \frac{p_1^2}{2m} + \frac{p_2^2}{2m} - \frac{1}{2}k(x_1^2 + x_2^2) + \frac{1}{2}\tilde{k}(x_1^4 + x_2^4) - \frac{1}{2}k_0(x_1 - x_2)^2 + \frac{1}{4}\tilde{k}_0(x_1 - x_2)^4. \tag{1}$$

Using Hamilton equations we obtain[1]:

$$\begin{cases} \dot{x}_1 = p_1/m, \\ \dot{p}_1 = kx_1 - \tilde{k}x_1^3 + k_0(x_1 - x_2) - \tilde{k}_0(x_1 - x_2)^3 + \varepsilon_1 \Gamma \cos(\omega t) - \varepsilon_2 T_1(p_1/m - w), \\ \dot{x}_2 = p_2/m \\ \dot{p}_2 = kx_2 - \tilde{k}x_2^3 - k_0(x_1 - x_2) + \tilde{k}_0(x_1 - x_2)^3 - \varepsilon_3 T_2(p_2/m - w) \end{cases} \tag{2}$$

where the perturbation terms have been added. The friction function is defined as follows:

$$T_i(p_i/m - w) = T_{i0}\mathrm{sgn}(p_i/m - w) - B_{i1}(p_i/m - w) + B_{i2}(p_i/m - w)^3 \tag{3}$$

where w is the tape velocity, whereas B_{11}, B_{12}, B_{21}, B_{22}, T_{10}, T_{20} are the friction coefficients. Introducing the following scaling

$$t \to t\sqrt{\frac{k}{m}}, \quad x = x_1\sqrt{\frac{\tilde{k}}{k}}, \quad u = p_1\sqrt{\frac{\tilde{k}}{mk^2}}, \quad y = x_2\sqrt{\frac{\tilde{k}}{k}}, \quad v = p_2\sqrt{\frac{\tilde{k}}{mk^2}} \tag{4}$$

and the following relations

$$k_0 = \xi k, \quad \tilde{k}_0 = \xi\tilde{k} \quad \text{where } \xi \geqslant 0, \tag{5}$$

[1] The dots over variables denote differentiation with time.

the analysed ODEs are cast in the nondimensional form

$$\begin{pmatrix} \dot{x} \\ \dot{u} \\ \dot{y} \\ \dot{v} \end{pmatrix} = \begin{pmatrix} u \\ x - x^3 + f_\xi(x,y) \\ v \\ y - y^3 - f_\xi(x,y) \end{pmatrix} + \begin{pmatrix} 0 \\ \varepsilon_1 \Gamma' \cos(\omega' t) - \varepsilon_2 T_1'(u - w') \\ 0 \\ -\varepsilon_3 T_2'(v - w') \end{pmatrix}, \tag{6}$$

where

$$T_1'(u - w') = T_{10}' \mathrm{sgn}(u - w') - B_{11}'(u - w') + B_{12}'(u - w')^3, \tag{7}$$

$$T_2'(u - w') = T_{20}' \mathrm{sgn}(v - w') - B_{21}'(v - w') + B_{22}'(v - w')^3, \tag{8}$$

$$\Gamma' = \Gamma \sqrt{\frac{\tilde{k}}{k^3}}, \quad \omega' = \omega \sqrt{\frac{m}{k}}, \quad T_{i0}' = T_{i0} \sqrt{\frac{\tilde{k}}{k^3}}, \quad B_{i1}' = \frac{B_{i1}}{\sqrt{mk}}, \quad B_{i2}' = \frac{k^2 B_{i2}}{\sqrt{m^3 \tilde{k}^3}}, \quad w' = w \sqrt{\frac{\tilde{k} m}{k^2}}, \tag{9}$$

$$f_\xi(x,y) = \xi(x - y) - \xi(x - y)^3.$$

Such system can be physically realized. Indeed, consider a system (see Fig. 1a) where a mass is connected via linear springs of the same stiffness κ_1. Due to the symmetry we can consider only one spring. Suppose, tha springs are initially compressed so that the mass is squeezed. Hence, when the mass is displaced there is a repulsive force acting on it:

$$F(x) = 2\Phi(x) \sin \alpha(x), \tag{10}$$

where $\Phi(x)$ is a linear force[2]:

$$\Phi(x) = \kappa_1 \left(r_0 - \sqrt{a^2 + x^2} - a \right), \quad \Phi(0) \equiv \Phi_o = \kappa_1 r_0. \tag{11}$$

For small displacements we can Taylor expand F:

$$F = \frac{2\kappa_1 r_0}{a} x - \frac{\kappa_1 x^3}{a^2}. \tag{12}$$

Hence, we can replace these two linear springs with one nonlinear spring (see Fig. 1b), which potential has the form:

$$V_1(x) = -\frac{\kappa_1 r_0}{a} x^2 + \frac{\kappa_1}{4a^2} x^4. \tag{13}$$

In a similar way we can obtain the potential for two masses:

$$V(x) = -\frac{\kappa_1 r_0}{a} x_1^2 + \frac{\kappa_1}{4a^2} x_1^4 - \frac{\kappa_1 r_0}{a} x_2^2 + \frac{\kappa_1}{4a^2} x_2^4 - \frac{\kappa_2 r_0}{a} (x_1 - x_2)^2 + \frac{\kappa_2}{4a^2} (x_1 - x_2)^4. \tag{14}$$

Applying the following substitutions:

$$k = 2\frac{\kappa_1 r_0}{a}, \quad \tilde{k} = \frac{\kappa_1}{a^2}, \quad k_0 = 2\frac{\kappa_2 r_0}{a}, \quad \tilde{k}_0 = \frac{\kappa_2}{a^2} \tag{15}$$

we get the same potential as in (1).

[2] Of course, the spring is linear in the extension along the spring.

3. The Melnikov-Gruendler's approach

The method applied in the paper is due to Gruendler (1985). Although the theory is a generalization to a non-Hamiltonian case we apply it to a Hamiltonian one. Here we consider a mechanical system governed by the equation:

$$\dot{x}(t) = f(x(t)) + h(x(t), t, \varepsilon), \tag{16}$$

where $f: R^4 \to R^4$ is a Hamiltonian vector field and $h: R^4 \times R \times B \subset R^4 \to R^4$ is periodic in t with frequency ω and satisfies $h(x(t),t,0) = 0$. For $\varepsilon = 0$ we obtain the unperturbed system. Let the unperturbed system possess a homoclinic orbit $\gamma(t)$ to a hyperbolic point at the origin. The variational equation along $\gamma(t)$ is the following:

$$\dot{y}(t) = Df(\gamma(t))y(t). \tag{17}$$

We seek a fundamental solution $\{\psi^{(1)}(t), \psi^{(2)}(t), \psi^{(3)}(t), \psi^{(4)}(t)\}$ to Eq. (17) possessing some special properties. The properties are the following:

(1) $\psi^{(4)}(t) = \dot{\gamma}(t)$[3].
(2) The initial vectors $\psi^{(i)}(0)$ span a vector space.
(3) Each $\psi^{(i)}(t)$ has the exponential behaviour as $t \to \pm\infty$. Namely:

$$\psi^{(i)}(t) \sim t^{k_i} e^{\lambda_i t} v^{(i)} \text{ as } t \to +\infty, \quad k_i \in N,$$

$$\psi^{(i)}(t) \sim t^{k_{\sigma(i)}} e^{\lambda_{\sigma(i)} t} \bar{v}^{(i)} \text{ as } t \to -\infty, \quad k_{\sigma(i)} \in N,$$

where σ is a permutation on four symbols and $\{\lambda_1, \lambda_2, \lambda_3, \lambda_4\}$ are the eigenvalues of $Df(0)$.
(4) The signs of $\Re(\lambda_i)$ and $\Re(\lambda_{\sigma(i)})$ in the exponential behaviour has to be such that:

$$\psi^{(1)}(t) = \begin{cases} \Re(\lambda_1) > 0, \\ \Re(\lambda_{\sigma(1)}) > 0, \end{cases} \tag{18}$$

$$\psi^{(2)}(t) = \begin{cases} \Re(\lambda_2) > 0, \\ \Re(\lambda_{\sigma(2)}) < 0, \end{cases} \tag{19}$$

$$\psi^{(3)}(t) = \begin{cases} \Re(\lambda_3) < 0, \\ \Re(\lambda_{\sigma(3)}) < 0, \end{cases} \tag{20}$$

$$\psi^{(4)}(t) = \begin{cases} \Re(\lambda_4) < 0, \\ \Re(\lambda_{\sigma(4)}) > 0. \end{cases} \tag{21}$$

Next we define an index set I by $i \in I$ if and only if $\psi^{(i)}(t) \overset{t \to \pm\infty}{\to} \infty$. Moreover we form the functions:

$$D(t) = \det\{\psi^{(1)}(t), \psi^{(2)}(t), \psi^{(3)}(t), \psi^{(4)}(t)\} e^{-\int_0^t \nabla f(\gamma(s)) \mathrm{d}s}. \tag{22}$$

[3] It is easy to show that $\dot{\gamma}(t)$ satisfies the Eq. (17).

Since f is a Hamiltonian vector field we obtain $\nabla f = 0$. Thus the function $D(t)$ reduces to simpler form:

$$D(t) = \det\{\psi^{(1)}(t), \psi^{(2)}(t), \psi^{(3)}(t)\psi^{(4)}(t)\}. \tag{23}$$

Let $K_{ij}(t, t_0)$[4] denote the result of replacing $\psi^{(i)}(t)$ in $D(t)$ by $\dfrac{\partial h(\gamma(t), t + t_0, 0)}{\partial \varepsilon_j}$. We define the function:

$$M_{ij}(t_0) = -\int_{-\infty}^{\infty} K_{ij}(t, t_0)\mathrm{d}t, \quad i \in I. \tag{24}$$

The function above measures the separation of stable and unstable manifolds. The Melnikov's function is defined as follows:

$$M(t_0) = \sum_{j=1}^{4} M_{ij}(t_0)\varepsilon_j, \quad i \in I. \tag{25}$$

4. The Melnikov–Gruendler's function

Let us denote by $\gamma(t)$ the homoclinic orbit of the point $\{0, 0, 0, 0\}$. It has (in our case) the following form

$$\gamma(t) = \begin{pmatrix} q(t) \\ \dot{q}(t) \\ -q(t) \\ -\dot{q}(t) \end{pmatrix}, \quad \text{where } q(t) = \sqrt{\frac{2(1+2\xi)}{1+8\xi}}\ \operatorname{sech}\left(t\sqrt{1+2\xi}\right). \tag{26}$$

The linearized system of the unperturbed equation (6) in vicinity of the homoclinic orbit $\gamma(t)$ reads

$$\dot{\psi} = F(t)\psi, \ \text{where } F(t) = \begin{pmatrix} 0 & 1 & 0 & 0 \\ 1+\xi-3(1+4\xi)q^2(t) & 0 & -\xi+12\xi q^2(t) & 0 \\ 0 & 0 & 0 & 1 \\ -\xi+12\xi q^2(t) & 0 & 1+\xi-3(1+4\xi)q^2(t) & 0 \end{pmatrix}. \tag{27}$$

Next we obtain the following equations

$$\begin{cases} \ddot{\psi}_1 = (1+\xi-3(1+4\xi)q^2(t))\psi_1 + \xi(12q^2(t)-1)\psi_3, \\ \ddot{\psi}_3 = (1+\xi-3(1+4\xi)q^2(t))\psi_3 + \xi(12q^2(t)-1)\psi_1. \end{cases} \tag{28}$$

A combination of Eq. (28) yields

$$\ddot{\phi}_1 = (1+2\xi)\left(1 - 6\operatorname{sec h}^2(t)\sqrt{1+2\xi}\right)\phi_1, \quad \phi_1 \equiv \psi_1 - \psi_3. \tag{29}$$

It is easy to see that $\psi^{(4)}(t) = \dot{\gamma}(t)$ satisfies the above equation. In order to find another solution, the following substitution is applied: $\dot{q}(t) \to r(t)\dot{q}(t)$. Since $\dot{q}(t)$ is a solution to (29) one gets

$$\ddot{r}\dot{q} + 2\dot{r}\ddot{q} = 0. \tag{30}$$

Integrating of (30) and owing to the obtained results, the solution reads

$$\phi_1(t) = r(t)\dot{q}(t)\left(\frac{3}{4}C_1 t - \frac{1}{2}C_1 ctgh(t) + \frac{1}{8}C_1\sinh(2t) + C_2\right)\dot{q}(t). \tag{31}$$

The above solution possesses the following asymptotics $\phi_1(t) \overset{t\to\pm\infty}{\to} \mathrm{e}^{\pm t\sqrt{1+2\xi}}$, so according to (19) we obtain the next solution $\psi^{(2)}(t)$. Next, summing up Eq, (28) we obtain

[4] This function represents the projection onto the direction of $\psi^{(i)}(t)$ of the ε_j of the h evaluated along $\gamma(t)$.

$$\ddot{\phi}_2 = g(t,\xi)\phi_2, \quad g(t,\xi) = 1 - 6\frac{1+2\xi}{1+8\xi}\,\mathrm{sec\,h}^2(t\sqrt{1+2\xi}), \quad \phi_2 \equiv \psi_1 + \psi_3. \tag{32}$$

Suppose that $y_1(t)$ is a solution of the above equation then $y_2(t) = y_1(-t)$ is also the solution because $g(t,\xi)$ is an even function with respect to t.

In our case, a perturbation term associated with (6) reads

$$h(t,\varepsilon) = \{0, \varepsilon_1 \Gamma' \cos(\omega' t) - \varepsilon_2 T_1'(u - w'), 0, -\varepsilon_3 T_2'(v - w')\}^{\mathrm{T}}. \tag{33}$$

Therefore, one gets[5]

$$\frac{\partial h(\gamma(t), t+t_0, 0)}{\partial \varepsilon_1} = \begin{pmatrix} 0 \\ \Gamma' \cos(\omega'(t+t_0)) \\ 0 \\ 0 \end{pmatrix}, \quad \frac{\partial h(\gamma(t), t+t_0, 0)}{\partial \varepsilon_2} = \begin{pmatrix} 0 \\ -T_1'(\dot{q}(t) - w') \\ 0 \\ 0 \end{pmatrix}, \tag{34}$$

$$\frac{\partial h(\gamma(t), t+t_0, 0)}{\partial \varepsilon_3} = \begin{pmatrix} 0 \\ 0 \\ 0 \\ -T_2'(\dot{q}(t) - w') \end{pmatrix}, \quad \frac{\partial h(\gamma(t), t+t_0, 0)}{\partial \varepsilon_4} \begin{pmatrix} 0 \\ 0 \\ 0 \\ 0 \end{pmatrix}. \tag{35}$$

Observe that only $K_{2j}(t,t_0)$ should be found, since $\psi^{(2)}(t) \overset{t\to\pm\infty}{\to} \infty$. First K_{21} is found

$$\begin{aligned} K_{21}(t,t_0) &= \det \begin{pmatrix} y_1 & 0 & y_2 & \dot{q} \\ \dot{y}_1 & \Gamma' \cos(\omega'(t+t_0)) & \dot{y}_2 & \ddot{q} \\ y_1 & 0 & y_2 & -\dot{q} \\ \dot{y}_1 & 0 & \dot{y}_2 & -\ddot{q} \end{pmatrix} \\ &= 2\Gamma' \dot{q} \cos(\omega'(t+t_0))(y_1\dot{y}_2 - \dot{y}_1 y_2) = 2(y_1\dot{y}_2 - \dot{y}_1 y_2)\Gamma' \dot{q} \cos(\omega'(t+t_0)). \end{aligned} \tag{36}$$

Second, K_{22} and K_{23} are found

$$K_{22}(t,t_0) = -2(y_1\dot{y}_2 - \dot{y}_1 y_2)\dot{q} T_1'(\dot{q} - w'), \quad K_{23}(t,t_0) = 2(y_1\dot{y}_2 - \dot{y}_1 y_2)\dot{q} T_2'(\dot{q} - w'). \tag{37}$$

Note that in each K_{2i} we have the same term $(y_1\dot{y}_2 - \dot{y}_1 y_2)$. It can be shown that $\Omega(\xi) = (y_1\dot{y}_2 - \dot{y}_1 y_2)$, i.e. this function is time-independent. Hence we obtain

$$K_{21}(t,t_0) = 2\Omega(\xi)\Gamma' \dot{q}(t) \cos(\omega'(t+t_0)), \tag{38}$$

$$K_{22}(t,t_0) = -2\Omega(\xi)\dot{q}(t) T_1'(\dot{q} - w'), \tag{39}$$

$$K_{23}(t,t_0) = 2\Omega(\xi)\dot{q}(t) T_2'(\dot{q} - w'). \tag{40}$$

[5] For more details see Section 3.

According to (24) we get

$$M_{21}(t_0) = -2\sqrt{2}\Gamma'\Omega(\xi)\pi\omega'\sqrt{\frac{1+2\xi}{1+8\xi}}\operatorname{sech}\left(\frac{\pi\omega'}{2\sqrt{1+2\xi}}\right)\sin(\omega' t_0). \tag{41}$$

$$\begin{aligned} M_{22}(t_0) &= 2\Omega(\xi)\int_{-\infty}^{\infty}\dot{q}T_1'(\dot{q}-w')\mathrm{d}t \\ &= 2\Omega(\xi)T_{10}'\int_{-\infty}^{\infty}\dot{q}\operatorname{sgn}(\dot{q}-w')\mathrm{d}t - 2\Omega(\xi)B_{11}'\int_{-\infty}^{\infty}\dot{q}(\dot{q}-w')\mathrm{d}t + 2\Omega(\xi)B_{12}'\int_{-\infty}^{\infty}\dot{q}(\dot{q}-w')^3\mathrm{d}t \\ &= -\frac{8}{3}\Omega(\xi)B_{11}'\frac{1+2\xi}{1+8\xi}\sqrt{1+2\xi} + \frac{32}{35}\Omega(\xi)B_{12}'\frac{(1+2\xi)^3}{(1+8\xi)^2}\sqrt{1+2\xi} + 8\Omega(\xi)B_{12}'w'^2 \\ &\quad\times\frac{1+2\xi}{1+8\xi}\sqrt{1+2\xi} + 2\Omega(\xi)T_{10}'\int_{-\infty}^{\infty}\dot{q}\operatorname{sgn}(\dot{q}-w')\mathrm{d}t. \end{aligned} \tag{42}$$

Consider the last integral in the above term:

$$\int_{-\infty}^{\infty}\dot{q}(t)\operatorname{sgn}(\dot{q}(t)-w')\mathrm{d}t = \frac{1+2\xi}{1+8\xi}\sqrt{1+2\xi}\int_{-\infty}^{\infty}\dot{\tilde{q}}(t)\operatorname{sgn}(\dot{\tilde{q}}(t)-\tilde{w}')\mathrm{d}t, \tag{43}$$

where $\dot{\tilde{q}}(t) = -\sqrt{2}\operatorname{sech}(t)\operatorname{tgh}(t)$ and $\tilde{w}' = w'\dfrac{\sqrt{1+8\xi}}{1+2\xi}$.

Assume first that $\tilde{w}' > 1/\sqrt{2}$, then

$$\int_{-\infty}^{\infty}\dot{\tilde{q}}(t)\operatorname{sgn}(\dot{\tilde{q}}(t)-\tilde{w}')\mathrm{d}t = \operatorname{sgn}(-\tilde{w}')\int_{-\infty}^{\infty}\dot{\tilde{q}}(t)\mathrm{d}t = 0. \tag{44}$$

Assume now that $\tilde{w}' < 1/\sqrt{2}$, then

$$\int_{-\infty}^{\infty}\dot{\tilde{q}}\operatorname{sgn}(\dot{\tilde{q}}-\tilde{w}')\mathrm{d}t = -\int_{-\infty}^{t_1}\dot{\tilde{q}}\mathrm{d}t + \int_{t_1}^{t_2}\dot{\tilde{q}}\mathrm{d}t - \int_{t_2}^{\infty}\dot{\tilde{q}}\mathrm{d}t = 2\sqrt{2}(\operatorname{sech}(\mathrm{t}_2) - \operatorname{sech}(\mathrm{t}_1)) \tag{45}$$

where

$$t_1 = \ln\left(\frac{1}{\tilde{w}'}\sqrt{1+\sqrt{1-2\tilde{w}'^2}}\left(1-\sqrt{\frac{1}{2}+\frac{1}{2}\sqrt{1-2\tilde{w}'^2}}\right)\right),$$

$$t_2 = \ln\left(\frac{1}{\tilde{w}'}\sqrt{1-\sqrt{1-2\tilde{w}'^2}}\left(1-\sqrt{\frac{1}{2}-\frac{1}{2}\sqrt{1-2\tilde{w}'^2}}\right)\right).$$

Substituting the obtained result we find

$$\begin{aligned} \frac{1+8\xi}{4(1+2\xi)^{3/2}}M_{22}(t_0) &= -\frac{2}{3}\Omega(\xi)B_{11}' + 2\Omega(\xi)B_{12}'\left(w'^2 + \frac{4(1+2\xi)^2}{35(1+8\xi)}\right) \\ &\quad + \Omega(\xi)T_{10}'\sqrt{2}\theta\left(\frac{1}{\sqrt{2}}-\tilde{w}'\right)(\operatorname{sech}(\mathrm{t}_2) - \operatorname{sech}(\mathrm{t}_1)), \end{aligned} \tag{46}$$

where $\theta(x)$ is Heaviside's function. In the similar way we obtain function $M_{23}(t_0)$. Finally, we find Melnikov–Gruendler function

$$M(t_0) = -\sqrt{2}\Gamma'\pi\omega'\operatorname{sech}\left(\frac{\pi\omega'}{2\sqrt{1+2\xi}}\right)\sin(\omega' t_0) - \frac{4(1+2\xi)}{3\sqrt{1+8\xi}}(B'_{11}-B'_{21}) + 4\sqrt{\frac{1+2\xi}{1+8\xi}}(B'_{12}-B'_{22})\left(w'^2+\frac{4(1+2\xi)^{5/2}}{35(1+8\xi)}\right) + 2\sqrt{2}(T'_{10}-T'_{20})\theta\left(\frac{1}{\sqrt{2}}-\tilde{w}'\right)\frac{1+2\xi}{\sqrt{1+8\xi}}(\operatorname{sech}(t_2)-\operatorname{sech}(t_1)). \quad (47)$$

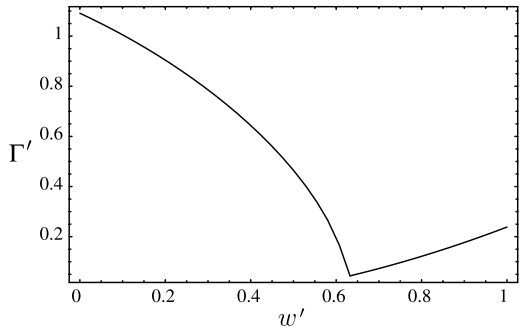

Fig. 2. The threshold curve.

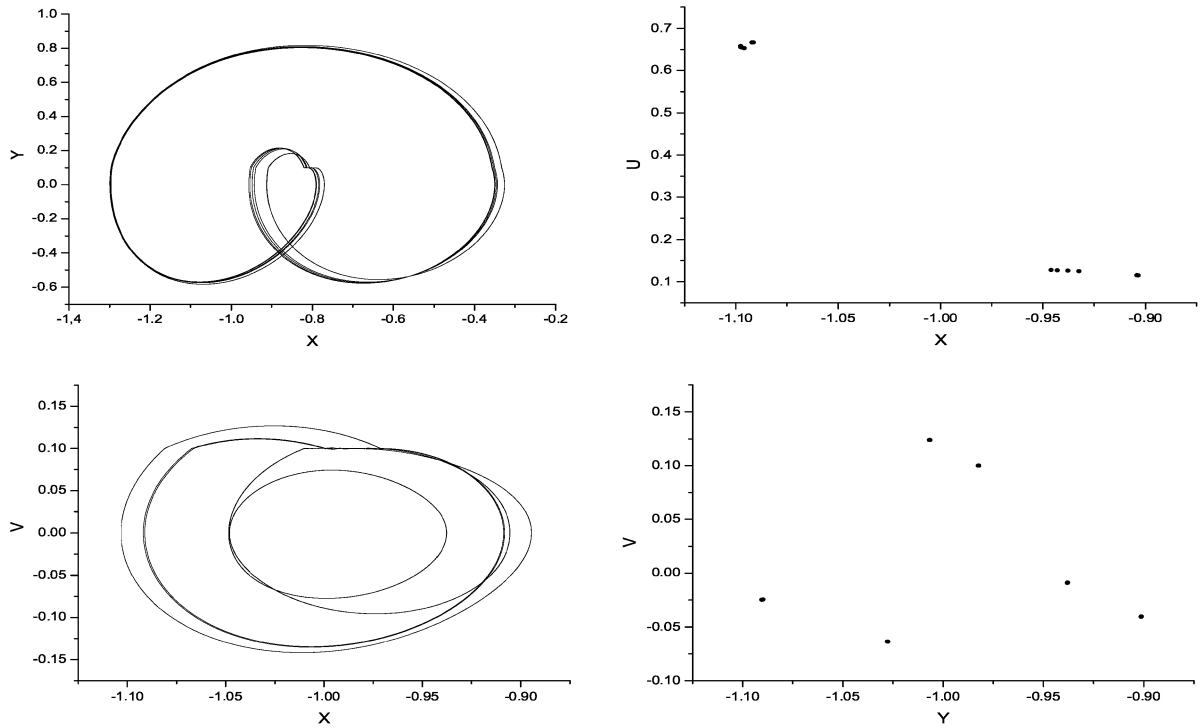

Fig. 3. $\Gamma' = 0.98$, $w' = 0.1$.

5. Numerical results

It is clear that having analytical form of the Melnikov's function various control parameters can be taken to show regular and/or chaotic dynamics. Let us take, following the paper (Awrejcewicz and Holicke, 1999), two of them i.e. $\{\Gamma', w'\}$ (see Fig. 2). The obtained curves define a chaotic threshold. Namely, above the mentioned curves chaos is expected, whereas below a regular behaviour is expected. The cusp corresponds to a switch between smooth and stick-slip dynamics. Note that the switch takes place exactly for the tape velocity value $w' = (1 + 2\xi)/(\sqrt{2}\sqrt{1 + 8\xi})$. One may state the following question. Why additional

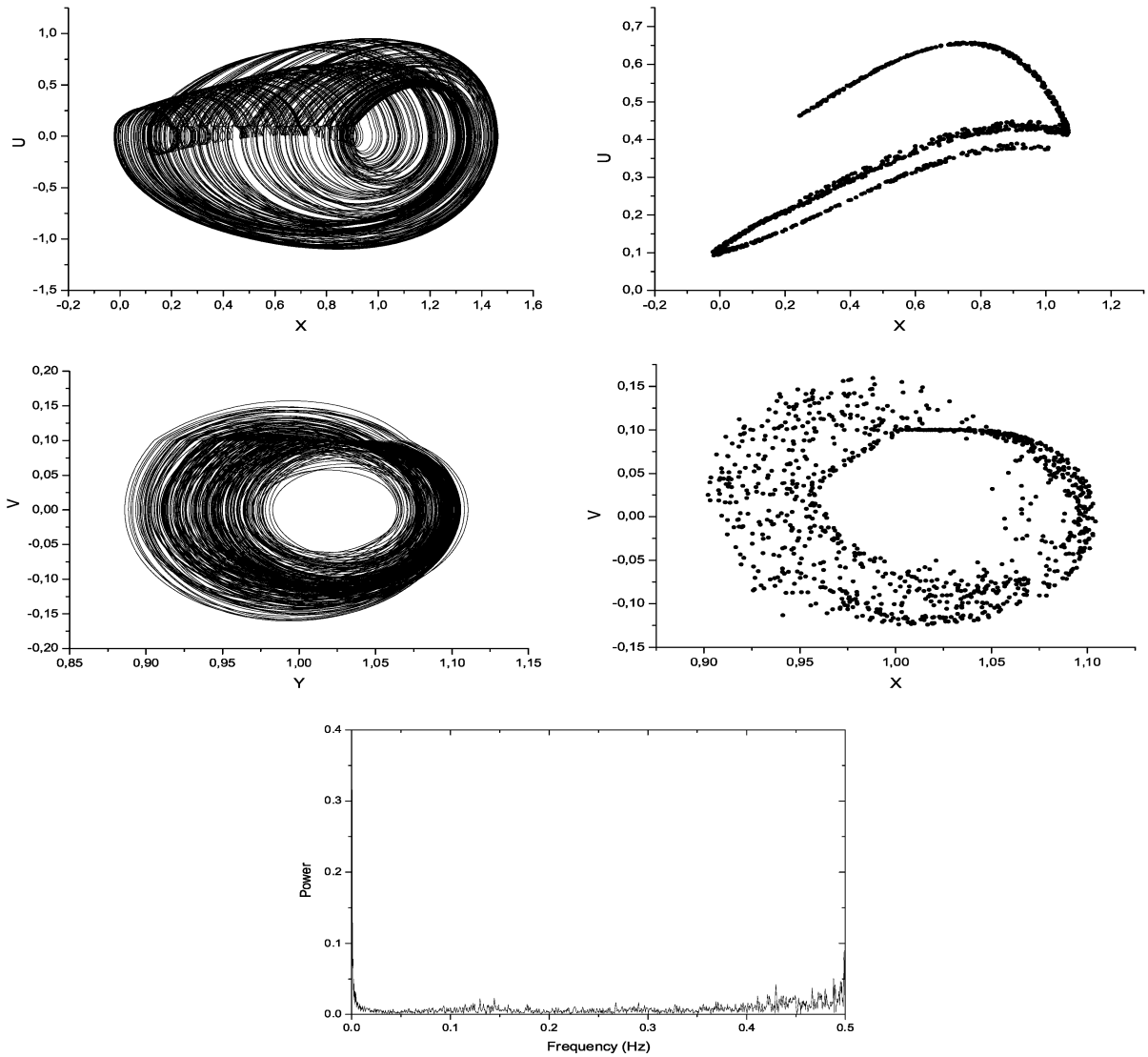

Fig. 4. $\Gamma' = 1.02$, $w' = 0.1$.

numerical examples are added having the analytical construction of the Melnikov's function. Some of the reasons are given below:

(i) It may happen that the obtained chaotic set is unstable, and hence it is impossible to show it applying a standard initial value problem.
(ii) Numerical tests allow for estimation of validity of our perturbational approach.
(iii) Numerical simulations can verify smooth and stick-slip chaotic dynamics. Note that in general approach given in reference (Gruendler, 1985), the introduced main theorem works only for C^2 systems.

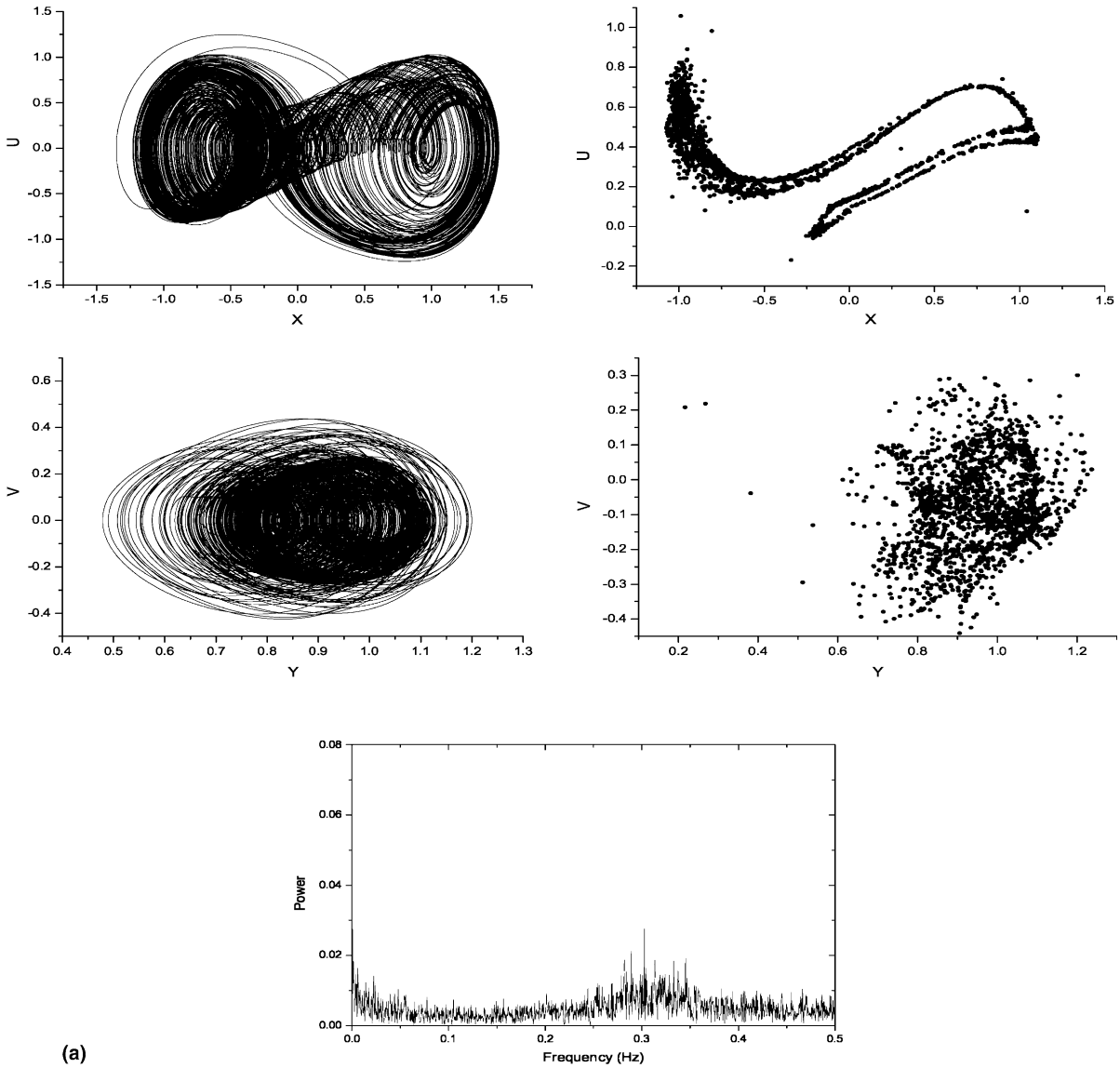

Fig. 5. (a) $\Gamma' = 1.1$, $w' = 0.1$ (b) $\Gamma' = 0.4$, $w' = 0.5$ and (c) $\Gamma' = 0.7$, $w' = 0.5$.

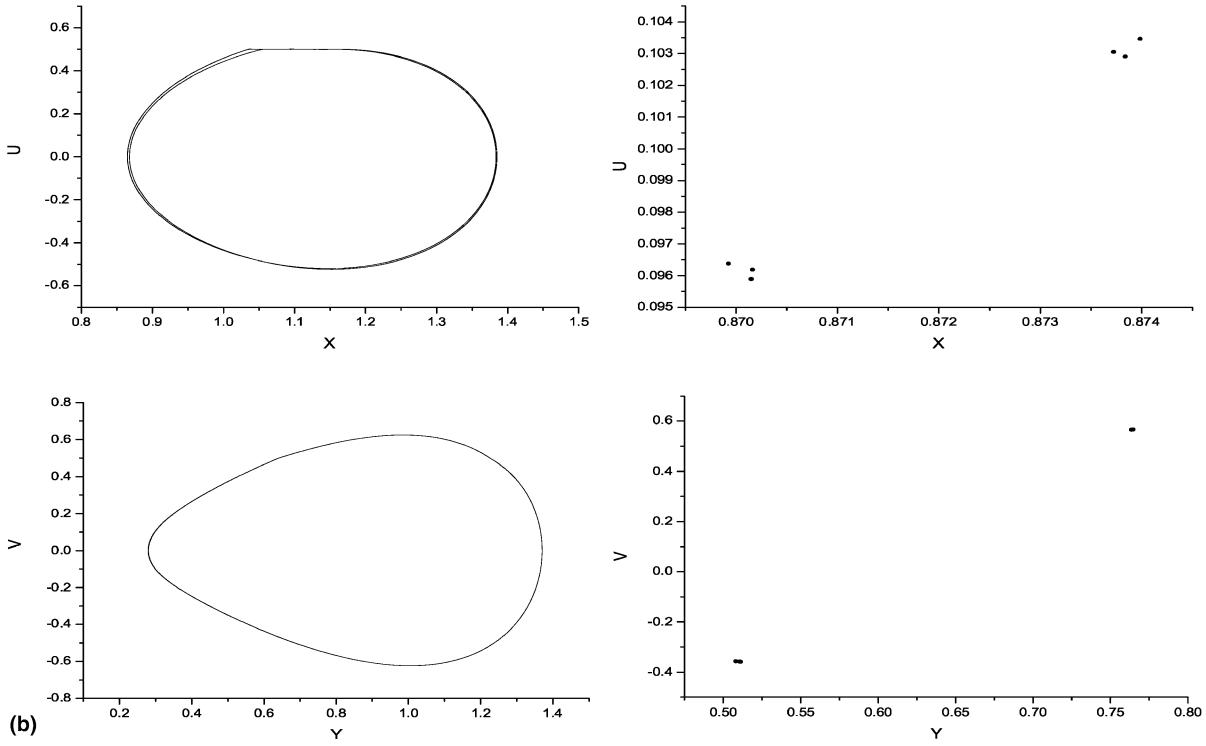

Fig. 5 (*continued*)

In our numerical simulations we have taken $T_{10} = 0.45$, $T_{20} = 0.05$, $B_{11} = 0.25$, $B_{21} = 0.15$, $B_{12} = 0.2$, $B_{22} = 0.1$, $\xi = 0.1$. The results are presented in the form of phase portraits (x, y), (y, v), Poincaré maps and power spectra (FFT) which correspond to the first block and the second one respectively. For $\{\Gamma' = 0.98,\ w' = 0.1\}$ we obtain periodic orbits (see Fig. 3). Observe that in these figures there are cusps which correspond to a sign change of the relative velocity. Moreover there are horizontal parts corresponding to the stick phases during the motion. While we cross the threshold curve we arrive at the point $\{\Gamma' = 1.02,\ w' = 0.1\}$, where qualitatively different behavior is observed (see Fig. 4). We can still observe stick phases during the motion (especially in (y, v) Poincaré section) and many cusps. Increasing Γ' to 1.1 chaotic behaviour is observed (see Fig. 5).

6. Concluding remarks

In this paper an important problem related to stick-slip chaos prediction is successfully solved. It possesses a challenging impact on analysis of all mechanical systems with friction, since many of them can be modelled by two degrees-of-freedom objects (Awrejcewicz and Lamarque, 2003). Motivated mainly by two papers (Awrejcewicz and Holicke, 1999; Gruendler, 1985), the homoclinic orbit is defined analytically, and then the Melnikov–Grunedler method is applied. The Melnikov's integrals are computed for both qualitatively different cases i.e. for regular and discontinous onset of chaos and the analytical prediction of chaotic threshold is verified by numerical computations.

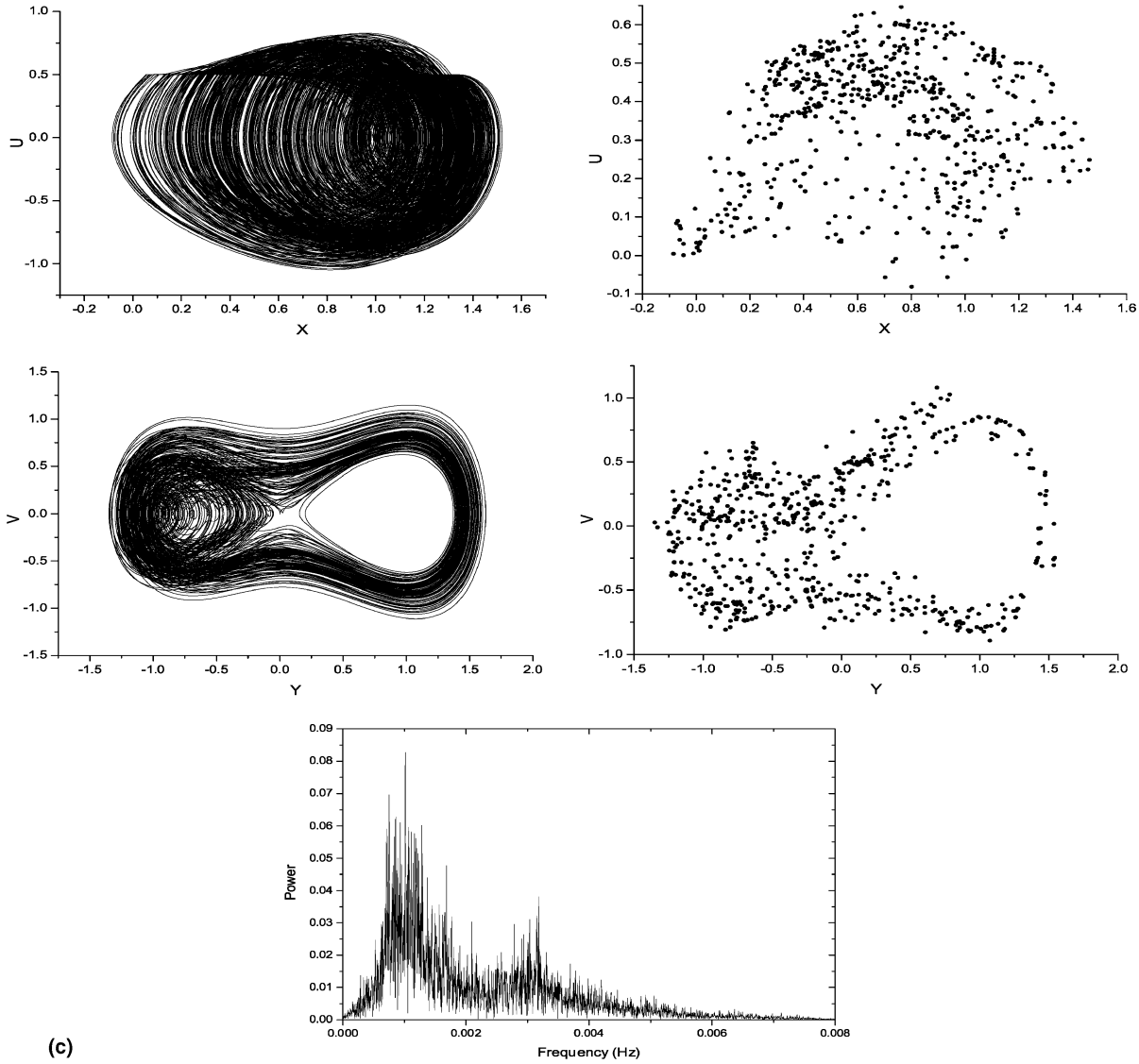

Fig. 5 (*continued*)

References

Awrejcewicz, J., Delfs, J., 1990. Dynamics of a self-excited stick-slip oscillator with two degrees-of-freedom. Part I. Investigation of equilibria. Eur. J. Mech. A/Sol. 9 (4), 269–282.

Awrejcewicz, J., Delfs, J., 1990. Dynamics of a self-excited stick-slip oscillator with two degrees-of-freedom. Part II. Slip-stick, slip-slip, stick-slip transitions, periodic and chaotic orbits. Eur. J. Mech A/Sol. 9 (5), 397–418.

Awrejcewicz, J., Holicke, M.M., 1999. Melnikov's method and stick-slip chaotic oscillations in very weakly forced mechanical systems. Internat. J. Bifur. Chaos 9 (3), 505–518.

Awrejcewicz, J., Lamarque, C.H., 2003. Bifurcations and Chaos in Nonsmooth Mechanical Systems. World Scientific, New Jersey, London, Singapore, Hong Kong.

Balasuriya, S., Mezic, I., Jones, C.K.R.T., 2003. Weak finite-time melnikov theory and 3D viscous perturbations of euler flows. Phys. D 176, 82–106.

Fathi, M.A., Salam, A., 1987. The Melnikov technique for highly dissipative systems. SIAM J. App. Math. 47, 232–243.
Fečkan, M., 1999. Chaotic solutions in differential inclusions: chaos in dry friction problems. Trans. Amer. Math. Soc. 351, 2861–2873.
Gelfreich, V.G., 1997. Melnikov method and exponentially small splitting of separatrices. Phys. D 101, 227–248.
Gruendler, J., 1985. The existence of homoclinic orbits and the method of Melnikov for systems in R^n. SIAM J. Math. Anal. 16, 907–931.
Holmes, P.J., Mardsen, J.E., 1982. Melnikov's method and Arnold diffusion for perturbations of integrable Hamiltonian systems. J. Math. Phys. 23, 669–675.
Kunze, M., 2000. Non-smooth dynamical systems Lecture Notes in Mathematics, 1744. Springer-Verlag, Berlin.
Lamarque, C.H., Bastien, J., 2000. Numerical study of a forced pendulum with dry friction. Nonlin. Dyn. 23, 335–352.
Melnikov, V.K., 1963. On the stability of the center for time-periodic perturbations. Trans. Moscow Math. Soc. 12, 1–56.
Pfeiffer, F., Hajek, M., 1992. Stick-slip motions of turbine blade dampers. Phil. Trans. R. Soc. London 338, 503–517.
Sanders, J.A., 1980. A note on the validity of Melnikov's method, Rep. 139, Wishundig Seminarium, Urije Universiteit, Amsterdam.
Smith, P., 1998. The multiple scales method, homoclinic bifurcation and Melnikov's method for autonomous systems. Int. J. Bifur. Chaos 8 (11), 2094–2105.
Stelter, P., 1992. Nonlinear vibrations of structures induced by dry friction. Nonlinear Dynam. 3, 329–345.
Sun, J.H., 1996. Melnikov vector function for high-dimensional maps. Phys. Lett. A 216, 47–52.
Weiyao, Z., Jiaowan, L., 1999. Exponential dichotomies and Melnikov functions for singularly perturbed systems. Nonlinear Anal. 36, 401–422.
Wiggins, S., 1989. Global Bifurcations and Chaos. Springer, Berlin.